Influence of Antenna Beamwidth on the Observed Characteristics of an Outdoor Vehicular Channel

Khalid A Al Mallak[1], Geoffery Hilton[1], Tian Hong Loh[2], Mark Beach [1]
[1] Communications Systems and Network, EPSRC CDT in Communications, University of Bristol (UoB)
Bristol, United Kingdom, {k.almallak, m.a.beach, geoff.hilton}@bristol.ac.uk
[2] Electromagnetic & Electrochemical Technologies Department, National Physical Laboratory/NPL,
Teddington, United Kingdom, tian.loh@npl.ac.uk

***Abstract*—Autonomous vehicles will require vehicle-to-vehicle (V2V) and vehicle-to-infrastructure (V2I) communications, which require very reliable, high-speed and low latency communications. Fifth-generation (5G) and beyond wireless networks become a solid base to build such infrastructure, using millimetre wave (mmWave) frequencies and beamforming techniques. The novelty of this paper is to investigate the influence of Doppler shift, Doppler spread and signal attenuation on a V2I communication channel employing a 26GHz phased array antenna from Anokiwave. This antenna facet acts as a spatial filter, eliminating unwanted multipath components (MPCs) and allowing the main beam to be electronically steered. The results show line-of-sight (LoS) communications between a base station (BS) and User Equipment (UE) for up to 150m distance for a transmitted power of 22dBm. A stable channel gain was observed during the measurements and related to the actual direction of the main beam. Further, the results indicated an attenuation between 78.2dB and 78.8dB when a vehicle obscures the LoS connection between the transmitter and the receiver. However, the appearance probability shows less attenuation experienced by the received signal when the phased array antenna employed a uniform beamwidth. Moreover, indirect communication, such as the non-line-of-sight scenario NLoS, is observed due to the reflections and scattering. Further, by driving the test vehicle in a car park with almost full of parked cars and at a speed of 5 mph, a very small Doppler shift was observed because of the suppression through spatial filtering from the array of the rich scattering and reflections within the environment.**

Index Terms— millimetre wave, antennas arrays, Beamforming, Doppler Shift/Spectrum, attenuation

I. INTRODUCTION

Innovative 5G communications technologies offering high data rates and low latency are well aligned to the connectivity needs of connected and autonomous vehicles (CAV). These applications require reliable vehicular communications for a vehicle to vehicle (V2V) or vehicle to infrastructure (V2I) data transmission. Recent work on millimetre-wave (mmWave) systems has shown a high data rate and low latency capability employing a steerable high directivity antenna facet at both the transmitter and the receiver [1]. Furthermore, beamforming via phased array antennas can thus electronically steer the beam such that the high directivity can be maintained appropriately [2, 3]. However, as the researcher is aware, there is no work done so far using a phased array antenna to investigate V2I communication at 26 GHz. However, many challenges exist, including vibrations produced from vehicular motion [4] as well as from passengers inside the vehicle [5]. This will cause both Doppler shift and Spread, degrading the quality of the communication of the channel. In addition, a greater degree of Doppler in the channel increases the complexity of signal tracking and demodulation [6].

The high bandwidth offered by the 26 GHz mmWave pioneer band [7] can be utilised for vehicular communications, increasing safety between vehicles in a move [1]. Therefore, to preserve a high bandwidth bearer, the channel gain must be stable [8, 9]. This is achievable by using phased array antennas to track the wanted signal and spatially filter unwanted directional signals, such as off-axis multipath components (MPCs) [10]. The successful deployment of mmWave for autonomous vehicles can confirm through the intensive research about the characterisations of a vehicular channel is necessary to investigate parameters that may directly influence the operation of communications bearers. This can be done through system-level simulations employing actuate and realistic channel models, with parameters extracted from real-world measurement campaigns.

This paper is divided into a theory section explaining how to compute the Doppler effect parameters using the time-frequency correlation. Then, the second section describes the measurements setup conducted at one site belonging to the University of Bristol (UoB). The results and analysis are presented in a third section giving results related to the characterisation of a vehicular channel. Finally, conclusions and recommendations are given.

II. BACKGROUND

A. Beamwidth of Phased Array Antennas

A phased array antenna is an antenna structure that combines multiple antenna elements and beamformer to the individual element excitation in terms of amplitude and phase. The main beam produced can be steered to the desired direction by changing the angle of departure (AoD) in azimuth elevation planes. According to [3, 11] beamwidth, of the main beam can be related to the coherence time, which is proportional to the Doppler shift. Therefore, by electronically steering the beam width, the impact of Doppler shift minimises.

B. Antenna mis-pointing

As mentioned earlier, to have reliable V2V or V2I communications, both Tx and Rx antennas are directional such that the narrow beam produced by the horn antenna or the phased array must be aligned to maximise the link budget. The phased array antenna can also act as a spatial filter, reducing the impact of off-axis MPCs and potentially vibration produced by motion [6, 12]. Moreover, the Doppler delay spectrum shown in [12] and seen in equation (1) below is based upon the Doppler shift, and the attenuation affected

DOI: http://doi.org/10.24086/cocos2022/paper.500

Figure 1: The site chosen for measurements 'Coombe Dingle Sport Complex' Loc1 & Loc2 showing two locations where the Tx was setup, the orange highlights show the paths used to take the measurements

the impulse response for a linear time-variant channel $h(t,\tau)$, which are influenced by the antenna mis-pointing because of the vibration. However, the Doppler Delay Spectrum (DDS) is computed by taking the Fourier transform of $h(t,\tau)$.

$$S(\tau, f_D) = \int_{-\infty}^{\infty} h(t,\tau)\, e^{-j2\pi f_D t} dt \qquad (1)$$

C. Channel gain and attenuation

A vehicular channel gain is a measure of the received power to transmitted power. This can show how stable the channel is during motion and beam tracking. The signal to noise ratio (SNR) is computed from the received signal strength indicator (RSSI), which is used on the other hand to compute the attenuation. The spatial dynamics of attenuation can be related to the channel correlation function. This includes the influence of the environment and embeds the Doppler activity in the channel. Furthermore, SNR can be improved by averaging Delay Doppler Spread over the excess delay τ_m [13] of the channel as shown in the following equation (2) [12] below:

$$\bar{S}(f_D) = \frac{1}{\tau_m} \sum_{\tau}^{\tau_m} S(\tau, f_D) \qquad (2)$$

D. Channel correlation function

It determines how the channel impulse response (CIR) observed from all MPCs are correlated. It is computed by using the CIR in the time domain and the frequency response in the frequency domain [14]. Depending on the type of the channel model, a vehicular channel has a correlation function which is computed from the measured CIRs after applying the cross-correlation function of the transmitted signal with the received signal. However, it is mathematically represented as shown in the integral equation (3) [12].

$$R_{xy}(\tau) = \int_{-\infty}^{\infty} x(t-\tau)^*.y(t)dt \qquad (3)$$

Where x*(t) and y(t) are the complex conjugates of the transmitted signal and the received signal correspondingly. As seen in previous work [14] the time-frequency correlation function is used to derive the temporal correlation which in the other hand used to compute the Doppler spectral density and other useful parameters for characterising a vehicular channel.

III. Measurements Setup

A phased array antenna used in the recent measurements conducted at the UoB showed very interesting results. Therefore, further measurements were arranged using the same phased array antenna to investigate V2I communications channel operating at 26GHz with 1GHz bandwidth. The measurements were performed at a site belongs to the UoB, namely, Coombe Dingle sports complex,

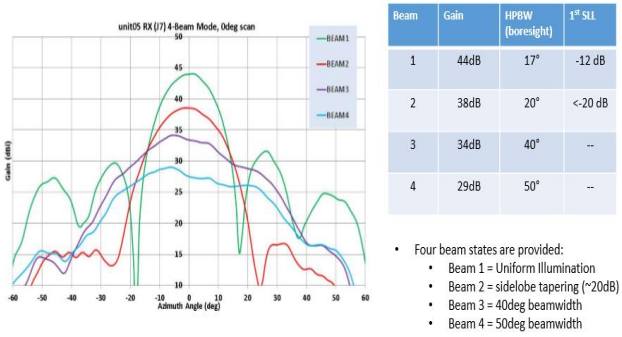

Beam	Gain	HPBW (boresight)	1st SLL
1	44dB	17°	-12 dB
2	38dB	20°	<-20 dB
3	34dB	40°	--
4	29dB	50°	--

- Four beam states are provided:
  - Beam 1 = Uniform Illumination
  - Beam 2 = sidelobe tapering (~20dB)
  - Beam 3 = 40deg beamwidth
  - Beam 4 = 50deg beamwidth

(a)

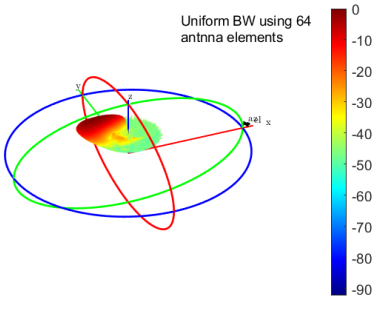

(b)

Figure 2: a & b Show the 2D and 3D radiation patterns for the Anokiwave phased array antenna correspondingly. 64 antenna elements mode was used to show the radiation pattern in elevation angle as in b for a uniform beamwidth.

DOI: http://doi.org/10.24086/cocos2022/paper.500

as seen in Fig. (1). The radiation patterns of the kit are depicted in Fig. (2) which shows the three Half Power Beam Width (HPBW) considered during the measurements. Only 64 antenna elements out of the 256 were used to transmit beamwidth of 17°, 20°, or 50°. The Rx antenna has an HPBW of 25°-17° nominal and a gain of (10-18)dBi. During one set of measurements, 3000 snapshots have been recorded every run to investigate the attenuation. Furthermore, 4000 snapshots were recorded during another set of measurements whilst the vehicle was moving and considering the three different beamwidths. In addition, the Doppler shift has been investigated for LOS and NLOS scenarios concerning the beamwidth.

As seen in Fig. (1), the site investigated has a long driveway with the main building and a good car park. Furthermore, a building of two stories on the left-hand side adds other environmental effects to the current setup. The UoB channel sounder was used to measure the CIR and frequency response using a 26GHz horn antenna at
the receiver side (Rx) and the Anokiwave phased array antenna at the transmitter's (Tx) side. All reflections, scattering and shadowing produced from the sites were recorded and used to analyse the interested vehicular channel parameters. For LoS scenario, the position of Tx was set at 'location 1' as shown in Fig. (1) using the kit at the height of 2 meters, while the RX antenna was mounted on the rack roof of a test vehicle that belongs to the UoB as shown in Fig. (1). The height of the vehicle is 1.485m, and the height of the rail is 9cm which makes the total height of the vehicle with the rack roof 1.575m. However, an additional bar was used to mount the Rx antenna, making the total height of the receiver's antenna 1.875m, including the bar fitted on the rack roof and used to mount the receiver's antenna on the roof of the roof vehicle.

The test vehicle was driven for 150 m along the 200 m driveway shown in Fig. (1) and at an allowable speed of 5miles/hour, corresponding to 2.24 m/s. Furthermore, 17° beamwidth was used during the measurements at this location. For NLoS, the same procedure was repeated, and both positive and negative Doppler shifts were investigated; however, the NLoS existed because Rx was 180° out of alignment with the transmitter. In the second scenario at location 2, the test vehicle was driven in the car park, and the same measurements were repeated for different beamwidth, namely, 17°, 20° and 50°. A final test was conducted on the same location to investigate the attenuation when a van of 4.55m length and 1.8m height obscured the LOS between Tx and Rx using only the 20° beamwidth.

IV. Results and Analysis

At location 1, the starting point was 5m away from the Tx antenna with some shadowing from the university van parked next to the transmitter, as seen in Fig. (1). The vehicle was driven away from Tx while Rx was facing the boresight of the transmitter. The Doppler shift was investigated in both scenarios, which showed some Doppler shifts because of the low ramps on the driveway, the few trees located on the left-hand side of the path, the lamppost, and the incoming and outgoing traffic as seen in Fig. (3). The last figure shows the Doppler impulse response, and the high peaks correspond to the Doppler shifts that are minor in the LoS scenario because the antenna acts as a spatial filter that suppresses the unwanted MPCs in a static environment. However, when

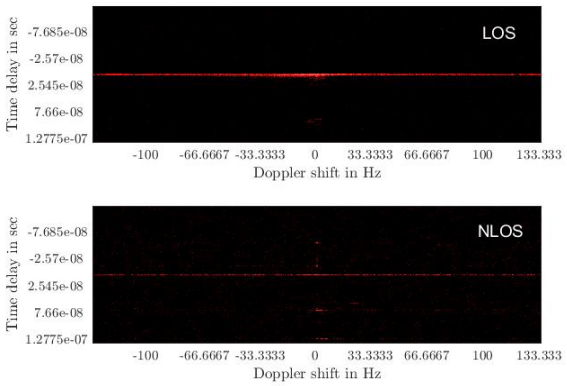

Figure 3: Doppler impulse response and Doppler shift for LOS/NLOS scenarios

NLoS was studied, a clear Doppler shift was seen due to the traffic observed during the measurements that created more MPCs to be recorded at Rx.

The Doppler shifts were calculated by taking a double Fourier transform of the recorded CIR through the channel sounder. Furthermore, the CIR was used to compute the Doppler impulse response as discussed in [3]. The frequency correlation function was used to characterise the vehicular channel over the travelled distance. It gives information about the channel's coherence bandwidth and how it changes over the travelled distance and differentiate between the LOS and the NLOS environments, as seen in Fig. (3). Further, because the channel is a frequency selective one, larger frequency correlation coefficients are related to the strong MPCs recorded at the receiver, which cause a higher coherence bandwidth as seen in LoS scenario. On the other hand, for the NLOS scenario, the frequency correlation coefficients were small because of the frequency characteristics which has an impact on the coherence bandwidth. Moreover, in LOS environment the frequency correlation coefficients were decreasing because Rx antenna misaligned with Tx antenna which reduces the received power. To maintain the received

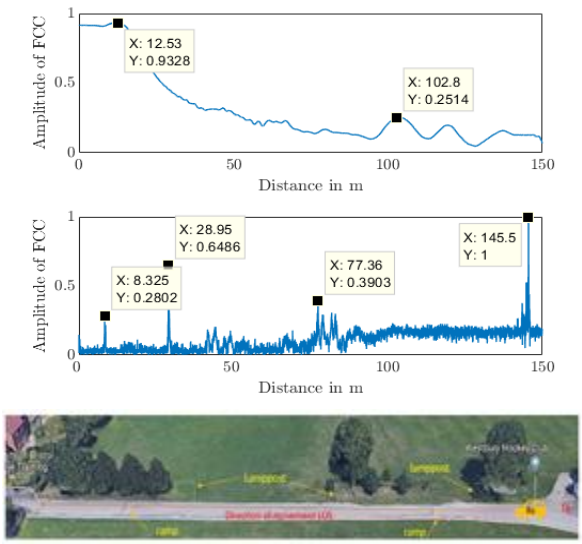

Figure 4: Frequency correlation function against the distance. It gives an idea about the coherence bandwidth and how it changed when the vehicle was moving away or towards Tx. The upper figure was for a LOS scenario while the middle figure was for a NLOS one. The lower figure shows the driveway where the measurements were performed with three lampposts and some trees.

power level at Rx, it would be better to steer the beam

DOI: http://doi.org/10.24086/cocos2022/paper.500

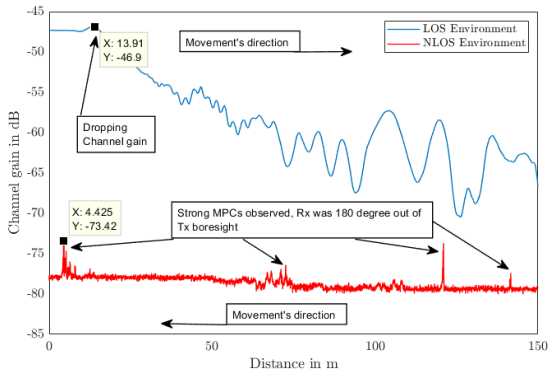

Figure 5: Shows channel gain in dB against the travelled distance of 150 m. The channel gain in NLOS was more stable than the LOS because there was no mis-pointing between Tx and Rx. The stability was characterised by having no steep drop in the channel gain when the vehicle moved away from Tx antenna as shown in the LOS scenario.

electronically so that the alignment would be maintained between Tx and Rx. frequency correlation coefficients were employed because of the small amplitudes computed from the double correlation of the time-frequency correlation function.

Fig. (4) presents some spikes observed in NLoS scenario, which can be explained as strong MPCs received by Rx because of the pedestrians, the lamppost, and the vehicles coming in and out to the sport complex. Moreover, in LoS scenario, the curve started with one, while in NLoS the curve started from near to zero because the normalisation was computed relative to the maximum amplitude of the frequency correlation function.

The antenna mis-pointing is an interesting phenomenon that became apparent at higher distances; hence the FCC became low. The mis-pointing causes a Doppler shift, and when it becomes incessant, the Doppler Spectrum will increase. Consequently, it will be more difficult for Rx antenna to distinguish between the MPCs.

A drawback is to consider out of these measurements; namely, the weather condition and the site's usability by the public restricted the performing of a reference measurement required to compare between the investigated scenarios. Therefore, some interruptions were inevitable during some measurements, but they were rectified through running more tests to complete the measurements. Without these drawbacks, the channel gain in LOS would be expected to be more stable, as seen in Fig. (5). From the last figure, it can be realised that

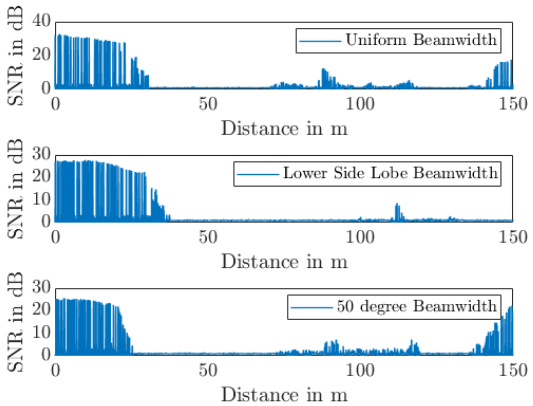

Figure 6: shows SNR against the distance for different beamwidths, which indicates 10 dB dynamic range in the results.

the channel's gain is

Beamwidth Parameter	Uniform (17°)	Low-Side-Lobe (20°)	50 °
Max SNR in dB	33.62	26.87	22.36

Table 1: SNR in dB relative to the travelled distance for different beamwidth of the phased array antenna.

related to the frequency correlation function shown in Fig. (4), which are computed from the CIR or the signal power. It can be understood that the shape of a vehicular channel's gain can be predicted from the vehicular channel correlation function or the received power. Furthermore, the low gain in NLoS scenario is related to a noise floor generated by Rx because the antenna was 180° out of alignment with the transmitter.

The second day of the measurement's campaign was conducted at location 2, as shown in Fig. (1). The Doppler shift was observed when the test vehicle was driven in a busy car park considering the three different beams mentioned earlier. The gains of 44, 38 and 29dBi of the phased array antenna depended upon the selection of the HPBW. In addition, the SNR was observed for the three beamwidths mentioned above, as shown in Fig. (6). It shows how the received power changes when the phased array antenna's operation mode changes. It also includes the gain of the antennas and the noise figure produced from the environment.

Further, high SNR of up to 33.62dB was observed when the beam was set on 17°, because the boresight was directed to the aperture of the Rx horn antenna, unlike the other beam observed where maximum SNRs were 26.87dB and 22.34dB for 20° and 50°, correspondingly. However, SNR dropped dramatically after travelling 35m because the path was utterly NLOS, and the only noise floor was observed. Moreover, after driving 75 m, only weak signals were picked up, which corresponded to the MPCs from the reflections produced from the parked vehicles.

Table (1) depicts the level of SNR produced for each beamwidth of the phased array antenna.

The attenuation is a parameter that characterises a vehicular channel. It shows how a mmWave responds when a vehicle obscures the LOS between BS and UE. For this experiment at location 2 and Fig. (7) a and b, a UoB van was parked between the Tx and Rx antennas. The Rx antenna was mounted again on the rack roof of the test vehicle. The chosen distances between the transmitter and the van were 6m and 12m. The attenuation was computed and presented against the recorded time to observe the influence of employing 20° beamwidth on the received power starting with a 6m distance from the transmitter antenna.

However, the same procedure was repeated for a 12m distance. The results indicate different MPCs recorded during the measurement in both scenarios produce different attenuations, as seen in Fig. (8), which were between 78.2-78.8dB, respectively. A deep look at the results showed there were other scatters around the direction of the specular reflections produced from the environment, increasing the received power as shown in [15] and reducing the attenuation. Most of the attenuation observed was when the received power was between -56dBm and -60dBm because of the ground reflections and reflections from the van's body and the environment.

DOI: http://doi.org/10.24086/cocos2022/paper.500

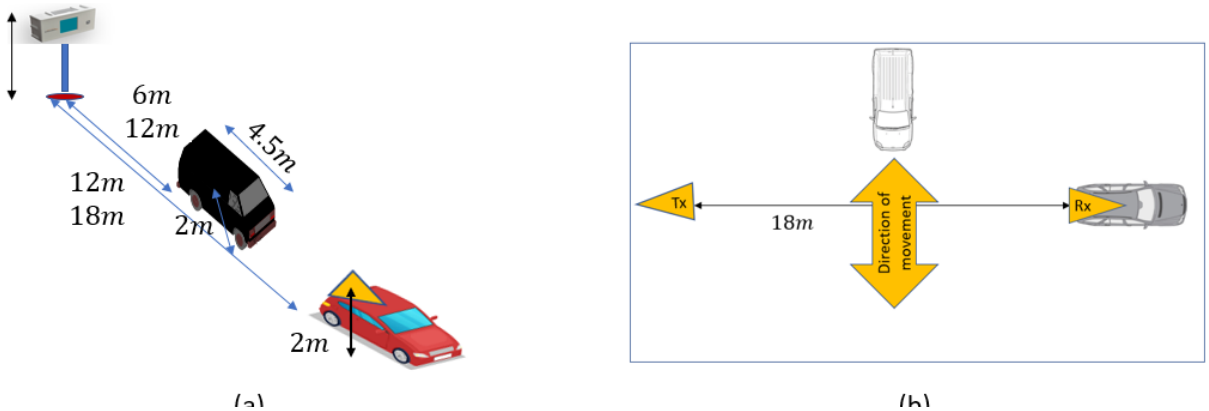

Figure 7: a & b show an image of the measurement performed and a measurement's plan to investigate the responses of the 26 GHz mm-wave when the van intersects the LOS between Tx and Rx.

These distances were chosen to validate a realistic scenario when a vehicle aims to communicate with a local BS, but another vehicle obscures the LoS connections. The results show a level of attenuation closed to the attenuation mentioned above when the van was 6 m away from Tx. Furthermore, for this attenuation, using a mmWave frequency in a vehicular channel can still maintain successful communication between a vehicle and infrastructure regardless of the obscuring van between the BS and UE.

A further measurement was performed at location 2, as shown in Fig. (7) b. It was aimed to investigate how a mmWave frequency responded when a van was intersecting the LoS between Tx and Rx by moving forward and reverse. The distance between Tx and Rx was 18 m, and the van was moving at a slow speed of 3mph. Further, the 17° and 20° HPBW were employed by the phased array antenna to investigate the attenuation computed using the same steps performed in the previous experiment. Further, the probability of appearance for the attenuation was computed and presented against the attenuation as depicted in Fig. (9). It shows significant attenuations observed in both scenarios that are comparable when the HPBW was changed from the uniform transmission into a low sidelobe one. Further, the van causes a blockage to the LoS; hence higher attenuation was observed when 20° HPBW was employed because of the ground reflections, scattering, and shadowing produced from the metal body and the glass windows of the van. Moreover, a probability of an appearance of around 20% was observed, corresponding to a complete blockage of the LOS by the van. Since the van was in motion, the probability mentioned above of appearance was steady while the attenuation was increased by 8dB over the intersecting time. As the van carried on reversing and moving forward, the probability of appearance increased with the attenuation as seen in Fig. (9).

V. Conclusion & Recommendation

This research continued the previous activity at the UoB that addresses the vehicular channel using the Anokiawave phased array antenna. The LOS and NLOS scenarios at location 1 exhibited a Doppler shift, unlike location 2. Here, the Doppler shift was very small because most of the MPCs were filtered by the directional antenna because of the narrow beamwidth of applied beam weights. Furthermore, the low sidelobe response yielded a high SNR necessary for V2I applications, as seen in Table (1). The measurements also characterised high attenuation observed when a van obscured and intersected the LOS between BS and UE.

Acknowledgment

This research was sponsored through the EPSRC CDT in Communications (EP/L016656/1) and NPL. The authors are also thanks both Anokiwave and Keysight technologies for their support.

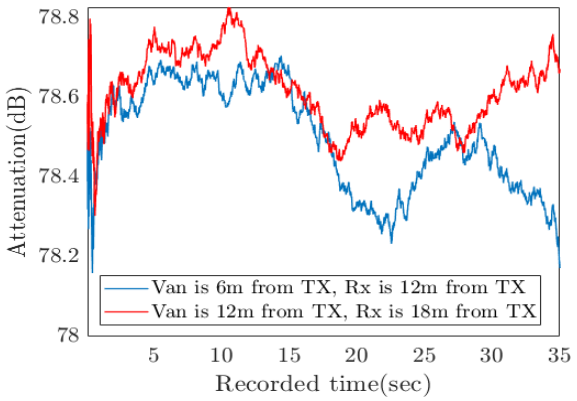

Figure 7: Presents the attenuation computed from the transmitted power and the received power relative to the recorded time. This corresponds to measurement's setup in Fig. (7) a. A lower sidelobe beamwidth of 20° was employed during that measurement. Higher attenuation was observed when the obscured van was 12 m away from Tx.

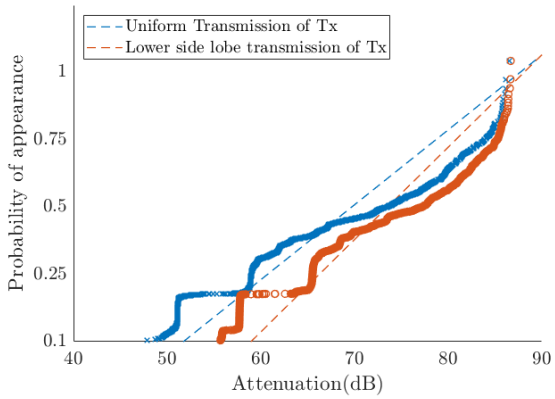

Figure 9: shows the computed probability of appearance relative to the attenuation observed when a van intersected the LoS between Tx and Rx and for both 17° and 20° HPBW Fig. (7) b.

DOI: http://doi.org/10.24086/cocos2022/paper.500

REFERENCES

[1] V. Petrov *et al.*, "The Impact of Interference From the Side Lanes on mmWave/THz Band V2V Communication Systems With Directional Antennas," *IEEE Transactions on Vehicular Technology*, vol. 67, no. 6, pp. 5028-5041, 2018.

[2] Z. Lin, X. Du, H. Chen, B. Ai, Z. Chen, and D. Wu, "Millimeter-Wave Propagation Modeling and Measurements for 5G Mobile Networks," *IEEE Wireless Communications*, vol. 26, no. 1, pp. 72-77, 2019.

[3] V. Va, J. Choi, and R. W. Heath, "The Impact of Beamwidth on Temporal Channel Variation in Vehicular Channels and Its Implications," *IEEE Transactions on Vehicular Technology*, vol. 66, no. 6, pp. 5014-5029, 2017.

[4] J. Blumenstein, A. Prokes, J. Vychodil, M. Pospisil, and T. Mikulasek, "Time-varying K factor of the mmWave vehicular channel: Velocity, vibrations and the road quality influence," in *2017 IEEE 28th Annual International Symposium on Personal, Indoor, and Mobile Radio Communications (PIMRC)*, 2017, pp. 1-5.

[5] E. Kampert, P. A. Jennings, and M. D. Higgins, "Investigating the V2V Millimeter-Wave Channel Near a Vehicular Headlight in an Engine Bay," *IEEE Communications Letters*, vol. 22, no. 7, pp. 1506-1509, 2018.

[6] A. Halimi, C. Mailhes, J.-Y. Tourneret, F. Boy, and T. Moreau, "Including Antenna Mispointing in a Semi-Analytical Model for Delay/Doppler Altimetry," *IEEE Transactions on Geoscience and Remote Sensing*, vol. 53, no. 2, 2015.

[7] M. Khalily, *26 GHz Indoor Wideband Directional Channel Measurement and Analysis in LoS and NLoS Scenarios*. 2018.

[8] T. Abbas, J. Nuckelt, T. Kürner, T. Zemen, C. F. Mecklenbräuker, and F. Tufvesson, "Simulation and Measurement-Based Vehicle-to-Vehicle Channel Characterisation: Accuracy and Constraint Analysis," *IEEE Transactions on Antennas and Propagation*, vol. 63, no. 7, pp. 3208-3218, 2015.

[9] S. Mukherjee, S. S. Das, A. Chatterjee, and S. Chatterjee, "Analytical Calculation of Rician K-Factor for Indoor Wireless Channel Models," *IEEE Access*, vol. 5, pp. 19194-19212, 2017.

[10] R. Sun *et al.*, "Millimeter-Wave Radio Channels vs. Synthetic Beamwidth," *IEEE Communications Magazine*, vol. 56, no. 12, pp. 53-59, 2018.

[11] V. Va and R. W. Heath, "Basic Relationship between Channel Coherence Time and Beamwidth in Vehicular Channels," in *2015 IEEE 82nd Vehicular Technology Conference (VTC2015-Fall)*, 2015, pp. 1-5.

[12] J. Blumenstein, J. Vychodil, M. Pospisil, T. Mikulasek, and A. Prokes, "Effects of vehicle vibrations on mmWave channel: Doppler spread and correlative channel sounding," in *2016 IEEE 27th Annual International Symposium on Personal, Indoor, and Mobile Radio Communications (PIMRC)*, 2016, pp. 1-5.

[13] V. Raghavan, A. Partyka, L. Akhoondzadeh-Asl, M. A. Tassoudji, O. H. Koymen, and J. Sanelli, "Millimeter Wave Channel Measurements and Implications for PHY Layer Design," *IEEE Transactions on Antennas and Propagation*, vol. 65, no. 12, pp. 6521-6533, 2017.

[14] V. S. Avramchuks and C. Tran Viet, "Time-frequency correlation analysis," in *International Forum on Strategic Technology 2010*, 2010, pp. 182-183.

[15] B. Antonescu, M. T. Moayyed, and S. Basagni, "Diffuse Scattering Models for mmWave V2X Communications in Urban Scenarios," in *2019 International Conference on Computing, Networking and Communications (ICNC)*, 2019, pp. 923-929.

DOI: http://doi.org/10.24086/cocos2022/paper.500